

6060

# **Molecular Modeling**

## **From Virtual Tools to Real Problems**

**Thomas F. Kumosinski, EDITOR**  
*U.S. Department of Agriculture*

**Michael N. Liebman, EDITOR**  
*Amoco Technology Company*

Developed from a symposium sponsored  
by the Division of Agricultural and Food Chemistry  
at the 205th National Meeting  
of the American Chemical Society,  
Denver, Colorado,  
March 28–April 2, 1993



American Chemical Society, Washington, DC 1994

## NMR and Molecular Modeling Evidence for Entrapment of Water in a Simple Carbohydrate Complex

P. Irwin, Gregory King, Thomas F. Kumosinski, P. Pieffer, J. Klein<sup>1</sup>,  
and L. Doner

Eastern Regional Research Center, Agricultural Research Service,  
U.S. Department of Agriculture, 600 East Mermaid Lane,  
Philadelphia, PA 19118

During structural investigations of a glucuronic acid derivative dissolved in DMSO we recognized a water activity-dependency between the NOESY cross-peaks of H<sub>2</sub>O and the carbohydrate's hydroxyl protons. The -OH↔H<sub>2</sub>O first order exchange rate constant increased from 0.32 to 11.14 s<sup>-1</sup> as the molar ratio of H<sub>2</sub>O:sugar increased from only ca. 4 to 5. The latter finding indicated that the -OH↔H<sub>2</sub>O proton exchange process, which is proportional to the translational diffusion of water, diminished as H<sub>2</sub>O approached the concentration which exists in the crystalline structure and was, presumably, entrapped by our glucuronic acid derivative forming a stable complex. Supporting this, a significant upfield shift in the resonance frequencies of the hydroxyl (-OH  $\Delta\delta_{\text{ave}} = 86.33$  Hz) protons was observed (CH  $\Delta\delta_{\text{ave}} = 0.25$  Hz) when water was removed by reaction with 2,2-dimethoxypropane. Molecular dynamics calculations (100 ps) on the energy-minimized carbohydrate-water complex confirm the presence of 2-3 near neighbor H<sub>2</sub>O molecules associated with the polar functional groups. In fact, the computationally-derived weighted average distance of all water molecules adjacent to the -OH groups was found to be inversely proportional to the individual -OH  $\Delta\delta$ s.

Knowledge about the interactions between carbohydrates and water is of some consequence because important chemical and physical properties are imparted by the way these compounds coexist. DMSO is a good solvent for understanding these interactions because carbohydrates retain much of their H<sub>2</sub>O-induced conformation (*1*) in DMSO and one can specifically observe, assign and study a carbohydrate's hydroxyl exchange with small quantities of H<sub>2</sub>O because the -OH resonance frequencies are dissimilar.

In this chapter we present spin-lattice relaxation, 2D NMR, chemical shift and molecular dynamics evidence that *N*-phenyl (*N*-phenyl- $\beta$ -D-glucopyranosylamine)-

uronamide's (*N*-phenyl uronamide; Figure 1) waters of crystallization are tightly bound to the polar functional groups of the sugar moiety even after extreme dilution in DMSO.

## Materials and Methods

**Sample Preparation.** *N*-phenyl uronamide was synthesized and purified as described previously (2,3). D-glucopyranuronic acid was dissolved in H<sub>2</sub>O (1.5 g/25 mL). Aniline (2 mL) was dropped slowly into the stirring mixture and the pH adjusted to 4.75 on a Radiometer (reference to brand or firm name does not constitute endorsement by the U. S. Department of Agriculture over others of a similar nature not mentioned) pH stat. Approximately 3 g of 1-ethyl-3-[3-(dimethylamino)propyl]carbodiimide (EDC) was added to the solution and the pH stat activated causing 0.1N HCl to be delivered to the reaction mixture to maintain the pH at ca. 4.75 (4-7). When no more titrant was needed to maintain a constant pH the reaction was complete. At this point an insoluble off-white precipitate had formed and was subsequently washed with H<sub>2</sub>O to remove unreacted aniline or EDC. Excess water was removed by washing the precipitate with chilled EtOH. The acid sugar derivative was then dissolved in hot EtOH and 2-4 mm needle-like crystals formed overnight at room temperature. For production of the anhydrous form, the above procedure was repeated except that a small amount of 2,2-dimethoxypropane was added to the EtOH to react with unwanted water (e.g., H<sub>2</sub>O + 2,2-dimethoxypropane → 2MeOH + acetone).

**NMR Spectroscopy.** Samples for NMR were prepared in a dry box. *N*-phenyl uronamide crystals were dissolved in DMSO-*d*<sub>6</sub> (≥ 99.5 atom % <sup>2</sup>H) which had been stored several days with molecular sieve pellets under dry N<sub>2</sub> (the DMSO contained, except when specified, ca. 30 mM H<sub>2</sub>O even in the presence of "dry" molecular sieves). Several DMSO-*d*<sub>6</sub> washed molecular sieves were kept in the 5 mm NMR tubes to maintain the sample in a relatively dry state; the NMR tubes were closed and wrapped with parafilm or sealed under vacuum to assist in the exclusion of extraneous H<sub>2</sub>O vapor. The samples were stored at 3°C and underwent no obvious degradative process, such as pyranose ring opening and associated Amadori rearrangement (2) or loss of the C<sub>1</sub> amine functionality (Figure 2). Evidence for water activity dependent hydrolysis (2) is provided in Figure 3. Using reverse phase HPLC, one can see that increasing the water concentration from ca. 0 to 50% (v/v) in MeOH increases the first order rate constant by a factor of about 9. It is noteworthy that there was a significant degree of hydrolysis (*t*<sub>1/2</sub> ~ 83 min) in absolute MeOH. For these kinetic experiments 3 mg of *N*-phenyl uronamide were dissolved in 10 mL of either 50% MeOH:H<sub>2</sub>O or abs. MeOH and maintained at 40°C. At various times 100 μL of each solution was injected into an HP 1090 HPLC system equipped with a supelco LC-18 reverse phase (15 cm; 5 μm particle size) column; 50 % MeOH was used as the mobile phase (0.2 mL min<sup>-1</sup>). The various peaks were checked against

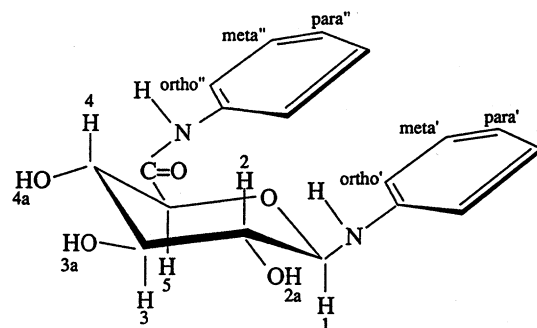


**Figure 1.** Structure and conformation *N*-phenyl uronamide  $^1\text{H}$  position labels.

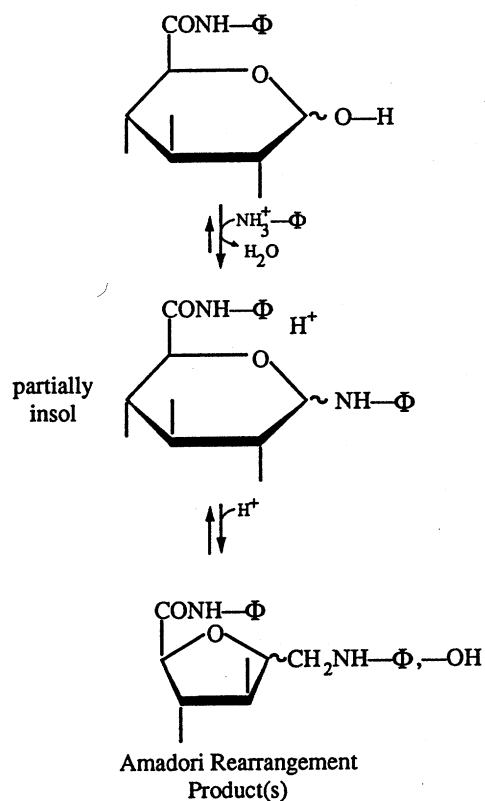


**Figure 2.** Reaction scheme proposed for the formation of *N*-phenyl uronamide and its Amadori rearrangement product(s). Reproduced with permission from Ref. 2. Copyright 1990, Journal of Carbohydrate Chemistry.

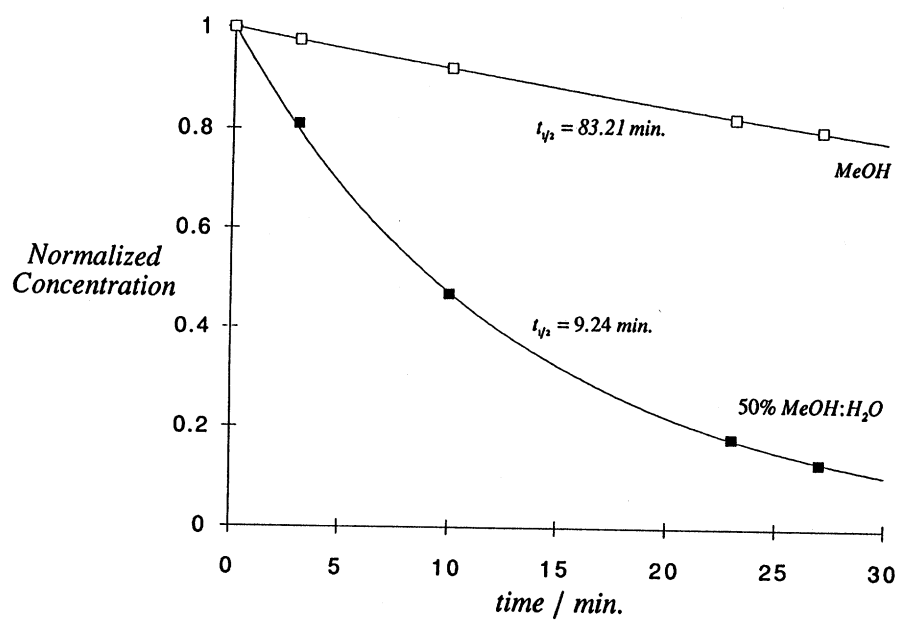


**Figure 3.** Change in the relative concentration of *N*-phenyl uronamide over time in 100% MeOH (open squares) and 50% MeOH:H<sub>2</sub>O (closed squares) at 40°C.

standards of aniline and *N*-phenyl-D-glucopyranuronamide (e.g., *N*-phenyluronamide without the C<sub>1</sub> amine functional group).

Before NMR experiments, the 90° pulse was determined for each condition, such as variable temperature or concentration, utilizing standard methods (8). All NOESY spectra were collected on a JEOL GX-400 NMR spectrometer system operated at ca. 400 MHz (9.40 T) using 5 mm probes (3). Computer line broadening was selected to be approximately equal to the digital resolution. These experiments were acquired using a matrix of 128 x 1024 (t<sub>1</sub> x t<sub>2</sub>), 256 x 2048 after zero-filling, complex data points which represented a spectral width of 953.1 Hz for either dimension. For each t<sub>1</sub> spectrum collected, 16 transients were acquired. A sine-bell apodization function was used to process these data. All quantitative 2D Overhauser enhancement matrices were processed without symmetrization. All ROESY (2) data were collected using a JEOL GSX-400 NMR spectrometer with a proton full-power 90° pulse of 10.5 μs. Acquisition data sets consisted of 2048 complex points for t<sub>2</sub> and 64 acquisitions for each t<sub>1</sub> data set. A spin-lock field of 3 kHz, 1 kHz off-resonance from the average chemical shifts of the residual H<sub>2</sub>O protons and the -OHs, was used for mixing times (τ<sub>m</sub>) of 0.075, 0.2, 0.4 and 0.6 s. The data sets were zero-filled to 4096 t<sub>2</sub> points and 2048 for t<sub>1</sub>. A phase-shifted sine-bell algorithm was used as the window function. All the -OH resonances (H<sub>2a</sub> → 4a) were integrated and fitted to an exponential function (equation 1)

$$I = I_o \left\{ 1 - e^{-\kappa \tau_m} \right\} \quad (1)$$

$$I_o = \lim_{\tau \rightarrow \infty} I \quad (2)$$

using a modified Gauss-Newton procedure developed in this laboratory by Dr. William Damert.

Proton T<sub>1</sub> inversion recovery experiments were performed on JEOL NMR spectrometers operated at either 400 or 270 MHz (9.40 or 6.34 T). Each τ value was signal averaged for 64 acquisitions with 16 dummy scans. T<sub>1sat</sub> experiments (9-11) were performed identically to the above except that the H<sub>2</sub>O resonance was irradiated 721.67 Hz upfield from the C<sub>4</sub>-OH (H<sub>4a</sub>) resonance. All peak intensity data were fit to an exponential function (equation 3) utilizing the aforementioned curve-fitting procedure.

$$I_i = I_o \left[ 1 - 2e^{\frac{-(\tau_i - \tau_o)}{T_1}} \right] \quad (3)$$

The T<sub>1sat</sub>-associated pseudo first-order rate constant (κ<sub>sat</sub>) calculation was

accomplished as shown in equation 4

$$\kappa_{sat} = \frac{1}{T_{1sat}} - \frac{I^+ / I^\phi}{T_{1sat}} \quad (4)$$

where  $I^+ / I^\phi$  is the ratio of hydroxyl resonance integrals with irradiation on the  $H_2O$  resonance and 721.67 Hz downfield, respectively.  $T_{1sat}$  is the normal  $T_1$  measurement but with spin saturation of  $H_2O$ .

The correlation time ( $\tau_c$ ) for the *N*-phenyl uronamide· $H_2O$  complex and individual resonance  $T_{1i}$  ( $T_{1i}$ ) were estimated using equation 5

$$\frac{1}{T_{1i}} = \frac{3}{10} \gamma^4 \left[ \frac{h}{2\pi} \right]^2 \sum_j \frac{1}{r_{ij}^6} \left\{ \frac{\tau_c}{1 + (\nu_o \tau_c)^2} + \frac{4\tau_c}{1 + (2\nu_o \tau_c)^2} \right\} \quad (5)$$

where  $\nu_o$  was either 270 or 400 MHz and the interproton distance parameter,  $r_{ij}$ , was assumed to be 2 Å since the interproton distance parameter has only a minor effect on the calculated  $T_{1i}$ s.

**Modeling Studies.** Initially, the SYBYL software package was used to construct the *N*-phenyl uronamide molecule and to prepare an initial dimer configuration (see Results and Discussion section). Certain dynamics simulations (Table III, Figure 9) were performed with the program SCHIZO which is a generalized version of the SCAAS model (12). In this model the solute is situated within a spherical droplet of solvent molecules and constraints are placed upon the solvent molecules near the surface of the sphere to prevent them from "evaporating" from the droplet. Other simulations (Figures 10 and 11) used the Sybyl software package alone as a comparison. Force-field parameters for bonding terms and nonbonded van der Waals interactions were from Clark and co-workers (13). Atomic charges for the carbohydrate and DMSO were obtained with the electronegativity equalization algorithm of Gasteiger and Marsili (14) except that the DMSO charges were subsequently scaled to make the dipole moment agree with the experimental value. For the SCHIZO model, all water force-field parameters were taken from King and Warshel (12); molecular dynamics trajectories were propagated using a 2 fs time step and "temperatures" were maintained at the desired values by utilizing gentle velocity scaling.

## Results and Discussion

*N*-phenyl uronamide is an unusual by-product of the activation of D-glucuronic acid's carboxyl group with a carbodiimide reagent (4-7) in the presence of the nucleophile aniline. Originally (2), the  $H_2O$  resonance was misassigned as the  $CH_3$  of DMSO since (Figures 2 and 3) the carbohydrate was found to be unstable

in the presence of free H<sub>2</sub>O and considerable effort (see Experimental) was taken to eliminate water from the samples. Other studies were performed because we supposed the observed cross peaks between the -OH groups and the "solvent" were due to magnetization transfer via spin diffusion or 2<sup>nd</sup> order Overhauser effects. However, upon treating *N*-phenyl uronamide with 2,2-dimethoxypropane (spectra shown in Figure 4) we discovered that this "solvent" peak disappeared and, therefore, was in fact a small amount of H<sub>2</sub>O which co-crystallized with the solute and/or which was absorbed from the head-space above the solvent (ca. 30 mM). When *N*-phenyl uronamide was recrystallized, as described previously, from hot EtOH without 2,2-dimethoxypropane and examined via <sup>1</sup>H NMR, using "100%" DMSO-*d*<sub>6</sub>, the H<sub>2</sub>O's of crystallization were found to exist in a ca. 4:1 molar ratio to the acid sugar derivative; upon vacuum drying at ca. 100°C the level of hydration could be reduced to 1 H<sub>2</sub>O:*N*-phenyl uronamide (C<sub>18</sub>H<sub>20</sub>O<sub>5</sub>N<sub>2</sub>·H<sub>2</sub>O; 3). A similar inaccuracy (*I*) may have been made on a similar-sized carbohydrate, cellobiose, inasmuch as comparable "DMSO"/-OH interactions (1<sup>st</sup> or 2<sup>nd</sup> order Overhauser effects), via NOESY NMR, have been hypothesized.

**Exchange and Exchange-like Phenomena.** In 2D Overhauser enhancement spectroscopic experiments, cross peaks not associated with scalar coupling result from either direct cross relaxation (15,16) or exchange phenomena (15-18). Direct cross relaxation (e.g., a "1<sup>st</sup> order Overhauser effect", 19) is a through-space dipolar spin-spin interaction proportional to the inverse 6<sup>th</sup> power of the distance between the interacting spins. Exchange-like phenomena (15-23) can be simplified as follows (3):

1. chemical exchange processes:
  - a. chemical exchange (15-18)
  - b. stereochemical exchange (17)
  - c. relayed exchange (18)
2. magnetization exchange processes:
  - a. "2<sup>nd</sup> order Overhauser effects" ( $\nu_0\tau_c \sim 1-10$ ; 19,21-23)
  - b. "spatial" and "spectral" spin diffusion ( $\nu_0\tau_c \gg 10$ ; 20)

The 2<sup>nd</sup> order Overhauser effects and other spin diffusion-like processes can only occur in solutions of molecules with relatively long  $\tau_c$ 's at high magnetic fields. Cellobiose, whose molecular weight (mw = 342.29) is similar to the title compound (mw = 344.36), is an unlikely candidate for any of the magnetization equilibrium processes listed above.

We became interested in the exchange behavior of the H<sub>2</sub>O:*N*-phenyl uronamide system since the water that was there was not acting as a catalyst for either the hydrolysis or Amadori rearrangement of our compound. Previous studies (Figure 3; 2) indicated that even minute quantities of water in MeOH induced a breakdown of about 36% per h. Thus, in the presence of up to 4-5 moles of water per mole of solute no breakdown was observed in DMSO over periods of several days indicating that the water was not available to interact under

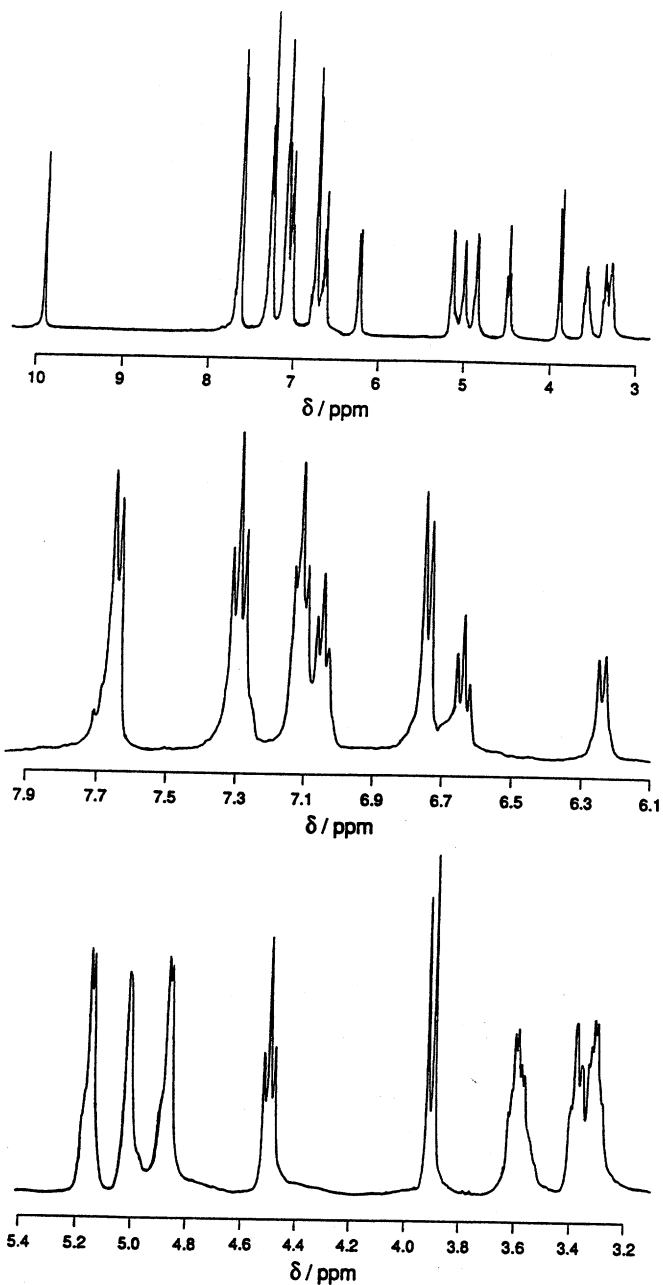


**Figure 4.**  $^1\text{H}$  NMR spectra of *N*-phenyl uronamide in the anhydrous state. For the hydrated form, a water resonance would appear, depending on the temperature, at ca. 3.34 ppm. Reproduced with permission from Ref. 3. Copyright 1993, Journal of Carbohydrate Chemistry.

these conditions. The rate of chemical exchange was measured from the mathematical behavior of off-diagonal -OH $\leftrightarrow$ H<sub>2</sub>O NOESY resonances as the mixing time ( $\tau_m$ ) was varied. For instance, during very slow chemical exchange (e.g., an amide-H,  $\tau_c = 0.1$ -5 ns; 18) NOESY cross peak integrals (I) should increase with mixing time ( $\tau_m$ ) as a typical 1<sup>st</sup> order rate process (equation 1) where I increases to a maximum, I<sub>0</sub>, as a function of  $\tau_m$  and eventually levels off; in this relation  $\kappa$  is a 1<sup>st</sup> order rate constant in units of reciprocal time. For <sup>1</sup>H donor species, similarly-sized to the above and displaying a moderate exchange rate, I increases to I<sub>0</sub> in a similar fashion to the above example but rapidly declines thereafter (18). NOESY data (Figure 5; all data points resulted from the integration of all off-diagonal -OH $\leftrightarrow$ H<sub>2</sub>O resonances) indicate that the H<sub>2</sub>O:*N*-phenyl uronamide complex underwent very slow exchange since I<sub>-OH/H<sub>2</sub>O</sub> stabilized as  $\tau_m$  approached 1 s. Also unusual was the fact that  $\kappa$  changed as a function of [H<sub>2</sub>O]:[*N*-phenyl uronamide]. Rotating frame 2D Overhauser (ROESY; 3,15,16,24) enhancement H<sub>1</sub> $\leftrightarrow$ H<sub>5</sub> cross peaks (Figure 6, upper spectrum) were negatively phased relative to the C<sub>2,3</sub> or 4-OH/H<sub>2</sub>O cross peaks (Figure 6, lower spectrum) thereby eliminating 1<sup>st</sup> order Overhauser effects as a possible explanation of our data. With regard to *N*-phenyl uronamide·4H<sub>2</sub>O, we found (Table I; 3) that  $\tau_c$  was ca. 0.54 ns via spin-lattice relaxation measurements at two fields. The calculated T<sub>1H</sub>s were observed to diverge from the experimental an average of only 0.48%. Clearly, based upon the  $\tau_c$  calculation and ROESY experiments the observed cross peaks between the solvating species, H<sub>2</sub>O, and the title compound's hydroxyl <sup>1</sup>Hs were due to chemical exchange. Further support for a slow exchange mechanism is presented in Figure 7 (3) whereupon inversion recovery experiments were performed with simultaneous irradiation at the H<sub>2</sub>O's resonance frequency (T<sub>1sat</sub>) and at an equivalent frequency off-set downfield (T<sub>1</sub>) from the observed hydroxyl proton (C<sub>4</sub>-OH). Based upon T<sub>1sat</sub> and I<sup>+</sup>/I<sup>0</sup> a  $\kappa_{sat}$  was found (equation 4) to be approximately 0.3 s<sup>-1</sup>. The process of longitudinal relaxation without exchange effects would be most nearly represented by the T<sub>1sat</sub> curve (open diamonds). The differences between these two treatments demonstrates the profound effect of exchange on the relaxation behavior of the -OH groups. Of course, magnetization equilibrium processes can be eliminated *a priori* as the basis of our observations since these processes occur only when  $\tau_c$ s for molecular reorientation are much longer (19,21-23).

As mentioned previously, we noted that the -OH $\leftrightarrow$ H<sub>2</sub>O exchange rate constant increased from 0.32 to 11.14 s<sup>-1</sup> as the molar ratio of [H<sub>2</sub>O]:[*N*-phenyl uronamide] increased only from ca. 4.5 to 5.2 (Figure 8). This latter finding indicated that  $\kappa$ , which is proportional to the translational diffusion of H<sub>2</sub>O (18), diminished as the water concentration approached that which was inherently complexed in the crystalline structure (C<sub>18</sub>H<sub>20</sub>O<sub>5</sub>N<sub>2</sub>·4H<sub>2</sub>O) and was, presumably, tightly hydrogen bound to the -OH and -NH functional groups when put into solution in DMSO. To further support this contention (Table II), the anhydrous

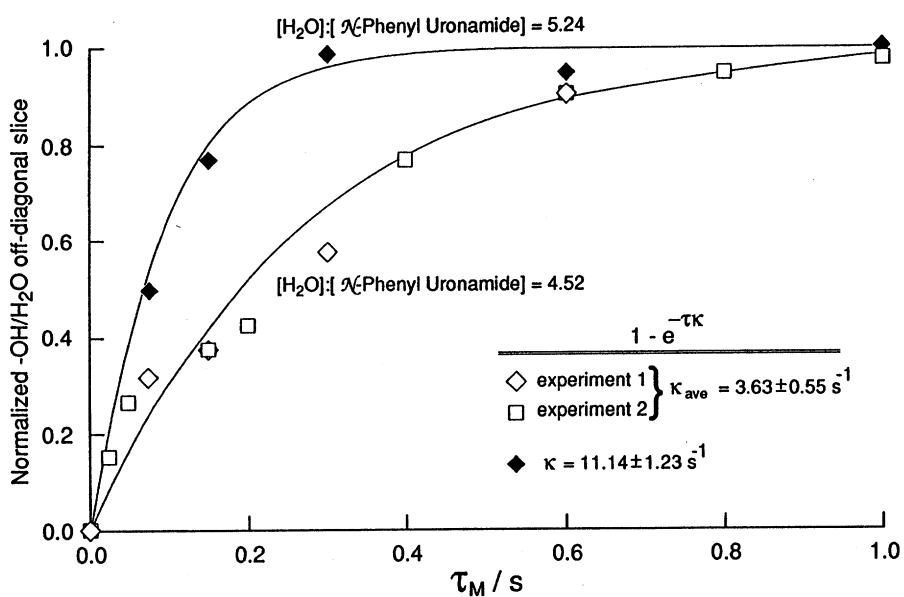


**Figure 5.** -OH $\leftrightarrow$ H<sub>2</sub>O cross peak areas plotted as a function of mixing time,  $\tau_m$ , at 40°C. Curves resulted from best fits to a first order exponential rate expression (equation 1). Reproduced with permission from Ref. 3. Copyright 1993, Journal of Carbohydrate Chemistry.

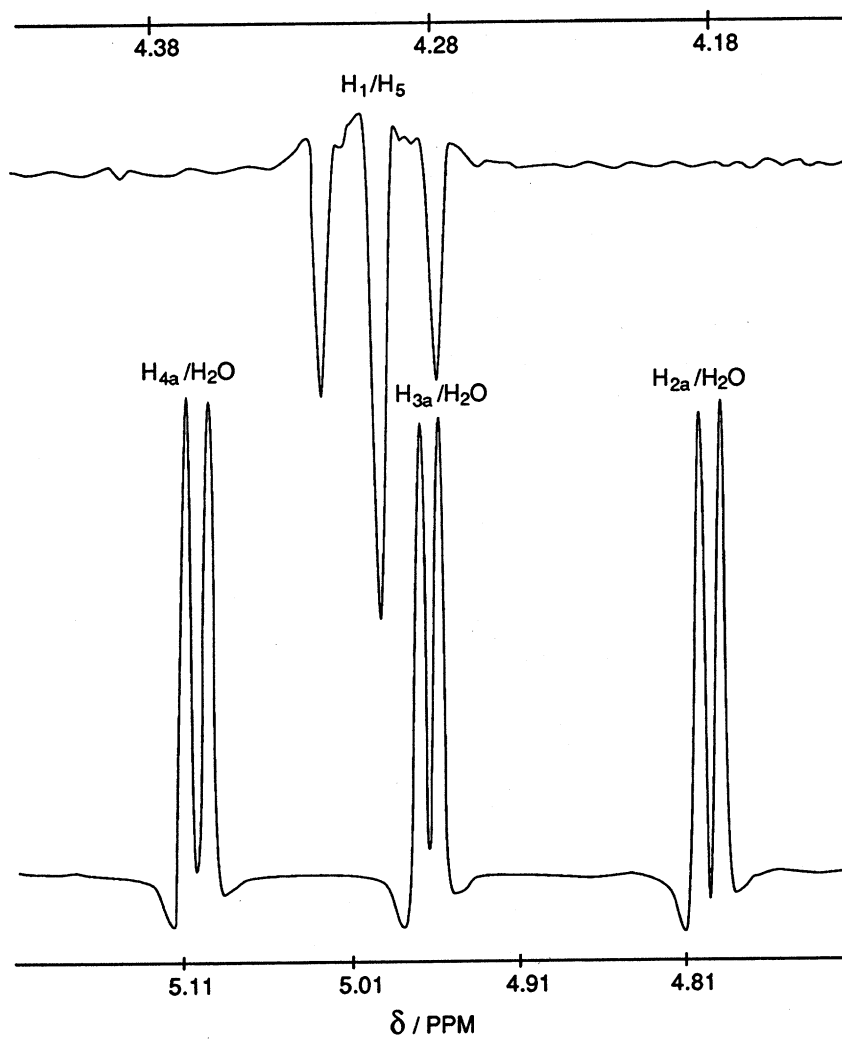


**Figure 6.**  $H_1 \leftrightarrow H_5$  and  $-OH \leftrightarrow H_2O$  ( $40^\circ C$ ) cross peaks from a ROESY experiment. Reproduced with permission from Ref. 3. Copyright 1993, Journal of Carbohydrate Chemistry.

version of the title compound was compared to *N*-phenyl uronamide·4H<sub>2</sub>O with respect to chemical shift changes ( $\Delta\delta$ ) upon dehydration. When no H<sub>2</sub>O was present in the DMSO/*N*-phenyl uronamide solution significant upfield

**Table I. Proton NMR spectral assignments and spin-lattice relaxation times (observed, calculated and difference) at 2 fields.**  
The correlation time ( $\tau_c = 5.4 \times 10^{-10}$  s) was based upon the static field dependence as shown in equation 5.

$\delta(^1H)$	$T_{1H}/s^a \{ \tau_c = 0.54ns \}$					
	270 MHz			400 MHz		
	obs. <sup>b</sup>	calc.	$\Delta$	obs.	calc.	$\Delta$
4.5 {C <sub>1</sub> -H}	0.25	0.32	0.07	0.61	0.57	-0.04
6.4 {C <sub>1</sub> -NH}	0.33	0.32	-0.01	0.56	0.57	0.01
5.34 {C <sub>2</sub> -OH}	0.84	0.83	-0.01	1.46	1.47	0.01
5.31 {C <sub>3</sub> -OH}	0.84	0.81	-0.03	1.42	1.44	0.02
5.01 {C <sub>4</sub> -OH}	0.85	0.79	-0.06	1.37	1.40	0.03
3.89 {C <sub>5</sub> -H}	0.31	0.41	0.10	0.77	0.72	-0.05
7.66 {Ortho"}	1.09	1.05	-0.04	1.84	1.86	0.02
7.29 {Meta"}	1.11	1.19	0.08	2.15	2.10	-0.05
7.04 {Para"}	1.59	1.46	-0.13	2.50	2.57	0.07
6.76 {Ortho'}	0.66	0.67	0.01	1.20	1.19	-0.01
7.11 {Meta'}	1.02	1.04	0.02	1.86	1.86	0.00
6.64 {Para'}	1.05	1.14	0.09	2.08	2.08	0.00

<sup>a</sup>42 mM solution at 40°C; see equation 5 for  $\tau_c$ - $T_{1H}$  calculation.

<sup>b</sup>All  $T_{1H}$  calculations had  $\leq 5\%$  error.

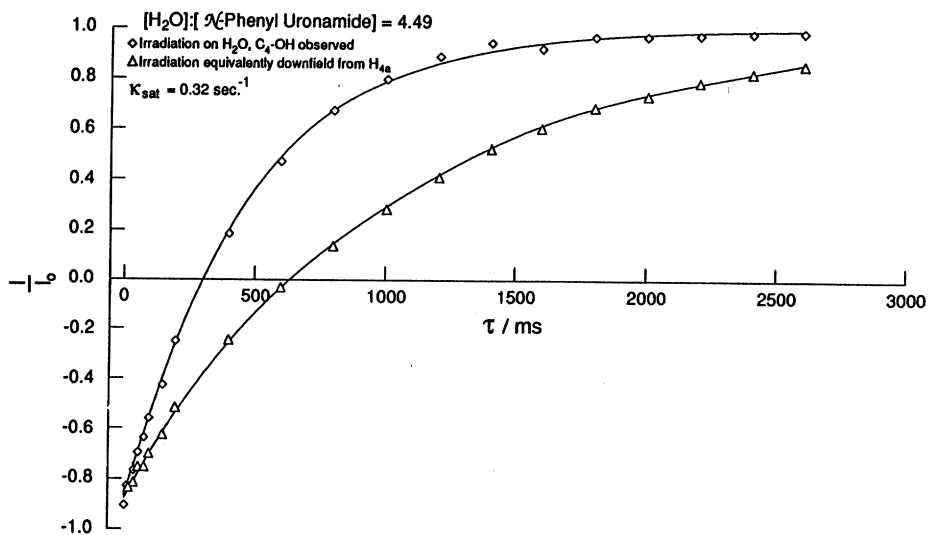


**Figure 7.** Inversion recovery experiments on *N*-phenyl uronamide (40°C; 400 mM;  $C_4\text{-OH}$  observed) with irradiation 721.67 Hz upfield (e.g., on the  $H_2O$  resonance) from  $C_4\text{-OH}$  (diamonds) and with the same treatment 721.67 Hz downfield from  $C_4\text{-OH}$  (triangles). Reproduced with permission from Ref. 3. Copyright 1993, Journal of Carbohydrate Chemistry.

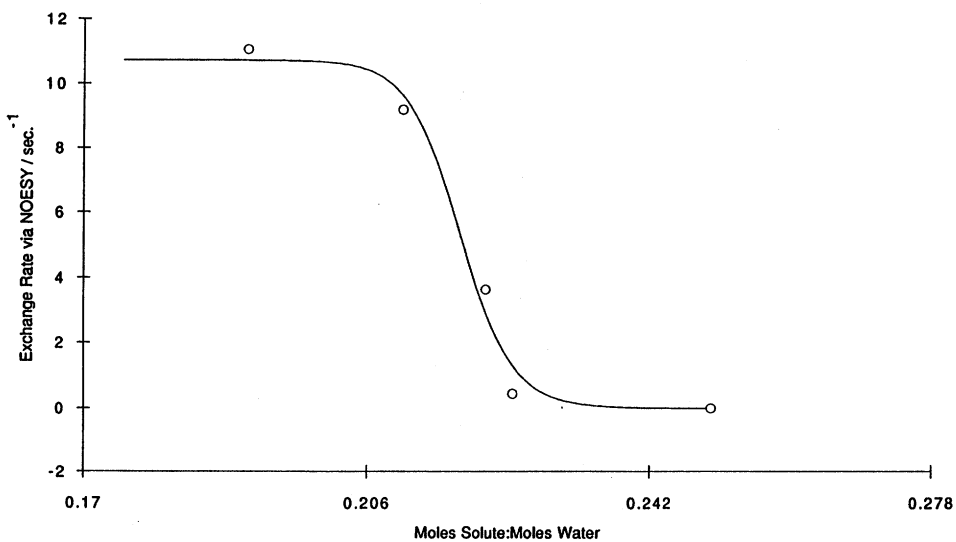


**Figure 8.** Plot of exchange rate constants as a function of  $[N\text{-phenyl uronamide}]:[H_2O]$  indicating extreme concentration of water dependence.

**Table II. Proton NMR spectral assignments for *N*-phenyl uronamide in the hydrated and dehydrated forms.**

Assignment	$\delta / \text{ppm}$		$\Delta\delta / \text{Hz}$
	[water] : [N-Phenyl Uronamide]		
	0:1	4:1	
Amide N-H <sup>a</sup>	9.91 <sup>b</sup>	10.09 <sup>c</sup>	72.00
Amine N-H	6.24	6.40	63.68
C <sub>4</sub> -O-H	5.14	5.34	78.40
C <sub>3</sub> -O-H	5.01	5.31	121.34
C <sub>2</sub> -O-H	4.86	5.01	59.24
			x = 78.93
Ortho"	7.64	7.66	6.34
Meta"	7.29	7.29	0.00
Para"	7.05	7.04	-2.28
Ortho'	6.75	6.76	5.42
Meta'	7.11	7.11	0.00
Para'	6.64	6.64	0.00
C <sub>1</sub> -H	4.50	4.50	0.00
C <sub>2</sub> -H	3.31	3.29	-7.64
C <sub>3</sub> -H	3.37	3.38	2.28
C <sub>4</sub> -H	3.59	3.60	4.32
C <sub>5</sub> -H	3.90	3.89	-5.74
			x = 0.25

<sup>a</sup>300 mM solution at 50°C; made with "100%" DMSO-*d*<sub>6</sub>.

<sup>b</sup>Reacted with 2,2-dimethoxypropane prior to crystallization.

<sup>c</sup>ca. 4.41 H<sub>2</sub>O molecules per molecule of *N*-phenyl (*N*-phenyl- $\beta$ -D-lucopyranosylamine)uronamide.

shifts on the resonance frequencies of all the polar (-OH  $\Delta\delta=86.33$  Hz; -NH  $\Delta\delta=67.84$  Hz) functional groups, relative to the methine protons (CH  $\Delta\delta=0.25$  Hz), were observed.

All these data are evidence that the water molecules in this system experienced the slowest exchange as the molar ratio of [H<sub>2</sub>O]:[*N*-phenyl uronamide] approached 4. Apparently, the translational diffusion of water, as measured by exchange, diminished dramatically as the molar ratio of H<sub>2</sub>O:*N*-phenyl uronamide approached that level bound in the crystalline structure and argues that the complex had a relatively long lifetime in solution. At the above levels of hydration most of the H<sub>2</sub>O might not be available for translational diffusion thereby causing  $\kappa$  to diminish. However, as H<sub>2</sub>O activity increased beyond the capacity of *N*-phenyl uronamide to bind it, the average residence time would necessarily diminish resulting in an elevation of  $k$  as a function of increasing the water concentration. At H<sub>2</sub>O levels well above 4:1 *N*-phenyl uronamide hydrolyses (2) to *N*-phenyl-D-glucopyranuronamide + aniline (Figures 2 and 3).

**Modeling the Behavior of H<sub>2</sub>O and *N*-Phenyl Uronamide.** We were interested in determining if molecular dynamics simulations would agree with our experimental observation that about 3-4 water molecules bind to *N*-phenyl uronamide with a long residence time even when in dilute solution. For this purpose, an *N*-phenyl uronamide dimer was constructed, energy minimized and placed in a sphere of water molecules with a radius of 12 Å. The temperature of the system was gradually raised from 0 to 300 K over 300 ps. At this point water molecules > 6 Å from the carbohydrate's polar groups were removed. The dimer and 33 water molecules were then placed in a sphere of DMSO (radius of 18.5 Å). The temperature was gradually raised from 0 to 300 K over 300 ps. After 50 ps at 300 K, the two sugars had drifted apart. The 2 monomers, with their neighboring water molecules, were separated into two new systems (Table III). One sugar had 8 water molecules within 6 Å of polar groups while the other had 10. The two systems were placed in new spheres of DMSO as before and the temperature was raised progressively to 300 K. At this point in time both of the sugars had 7 near-neighbor water molecules. After an additional 100 ps at 300 K both systems had 2-3 water molecules  $\leq 10$  Å of the polar functional groups, a number somewhat lower than expected from the NMR data (e.g., ca. 4). Assuming that the Interaction energy change ( $\Delta U_{\text{HB}}$ ) necessary to form one H-bond is ca. 5 kcal/mol then the ratio of all interaction Internal energy changes ( $\Delta U_{\text{I}}/\Delta U_{\text{HB}}$ ) calculated for our complex as a function of time should provide a measure of the number of interactions per water molecule. Table III shows that the near neighbor water molecules have a little over 1 H-bond with the polar functional groups of our carbohydrate model. However, showing better agreement with the NMR data was the observation that the weighted average distance ( $d$ ) of all water molecules the -OH groups was found to be inversely proportional (equation 6) to the individual -OH  $\Delta\delta$ s (Figure 9).

$$d = \sum_{j=1}^3 \frac{1}{r_j^3} \quad (7)$$

In this relationship the same 3 H<sub>2</sub>O molecules were used for the calculation depicted in Figure 9. A similar relationship was noted for the N-H functional groups. Other modeling studies using the SYBYL software package exclusively indicated (Figures 10 and 11) that the spatial variation of water molecules close to the polar functional groups was quite low (2.5-3Å) after 50 ps of simulated time.

**Table III.  $\Delta U_{\text{Interaction}}$  and  $\Delta U_{\text{Interaction}}/\Delta U_{\text{Hydrogen Bond}}$  calculations on the H<sub>2</sub>O:*N*-phenyl uronamide complex as a function of time at 300K.**

<i>System</i>	<i>Time (ps) after warmup to 300K</i>	$\Delta U_I/\text{kcal mol}^{-1}$	$\frac{\Delta U_I}{\Delta U_{HB}}$	$H_2O \leq 10\text{\AA}$
Monomer 1	0	-32.5	6.5	7
	50	-29.4	5.9	4
	100	-25.3	5.2	3
Monomer 2	0	-36.3	7.3	7
	50	-12.4	2.5	3
	100	-9.9	1.9	2

### Conclusions

NMR experiments indicate that a stable complex of approximately 4:1 H<sub>2</sub>O:*N*-phenyl uronamide exists even with extreme dilution in DMSO. Evidence for this was: a) the carbohydrate underwent no obvious hydrolysis in the presence of these hydration waters; b) the rate of chemical exchange was slower than one would expect for a -OH $\leftrightarrow$ H<sub>2</sub>O interaction; c) there was a concentration of water dependence for the exchange rate constant; d) upon dehydration of the complex there was a large chemical shift change in the polar functional groups. The molecular modeling studies were found to agree with the NMR results since the weighted average distance of all water molecules the -OH groups was found to be inversely proportional to the individual -OH  $\Delta\delta$ s.

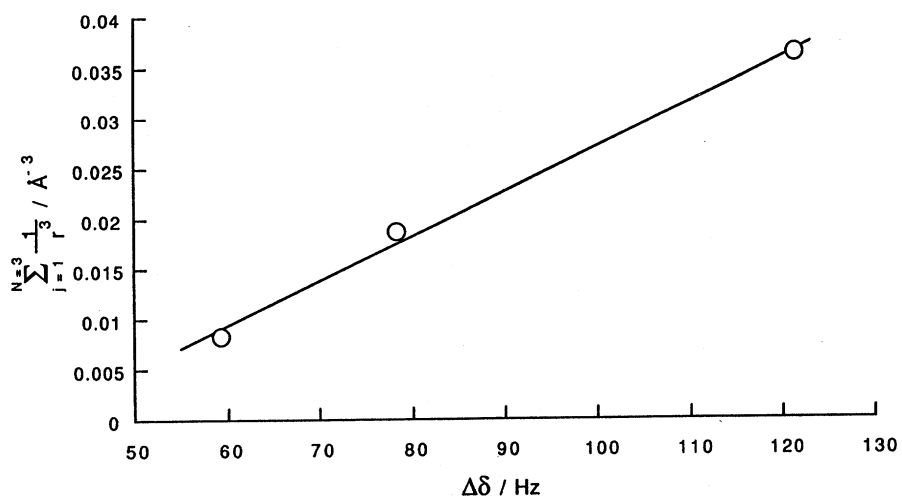


**Figure 9.** Plot of reciprocal weighted average distance of all water molecules the -OH groups, from dynamic simulations, as a function of individual -OH  $\Delta\delta$ s.

Reprinted from ACS Symposium Series No. 576  
*Molecular Modeling: From Virtual Tools to Real Problems*  
 Thomas F. Kumosinski and Michael N. Liebman, Editors  
 Copyright © 1994 by the American Chemical Society  
 Reprinted by permission of the copyright owner

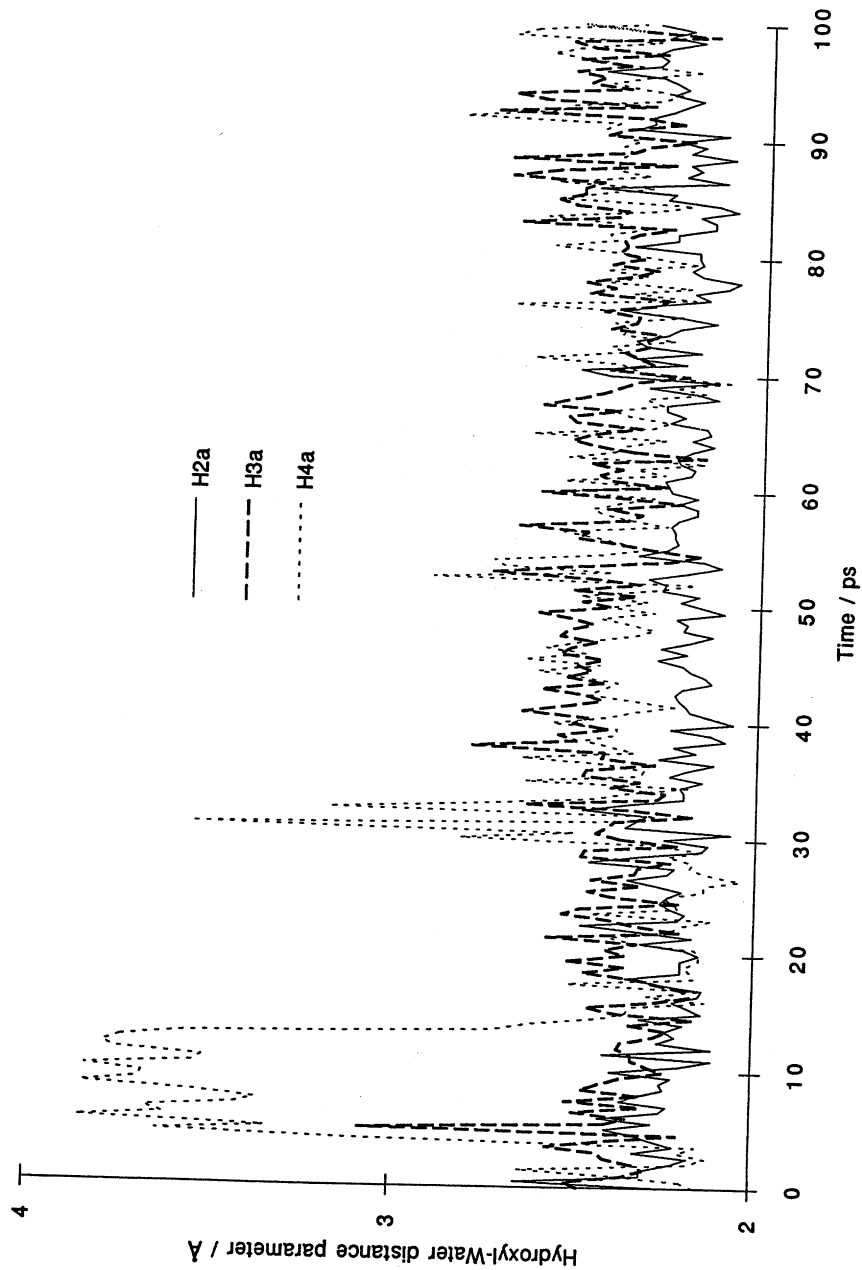


**Figure 10.** Variation of *N*-phenyl uronamide -OH $\leftrightarrow$ H<sub>2</sub>O distances as a function of simulated time in DMSO.

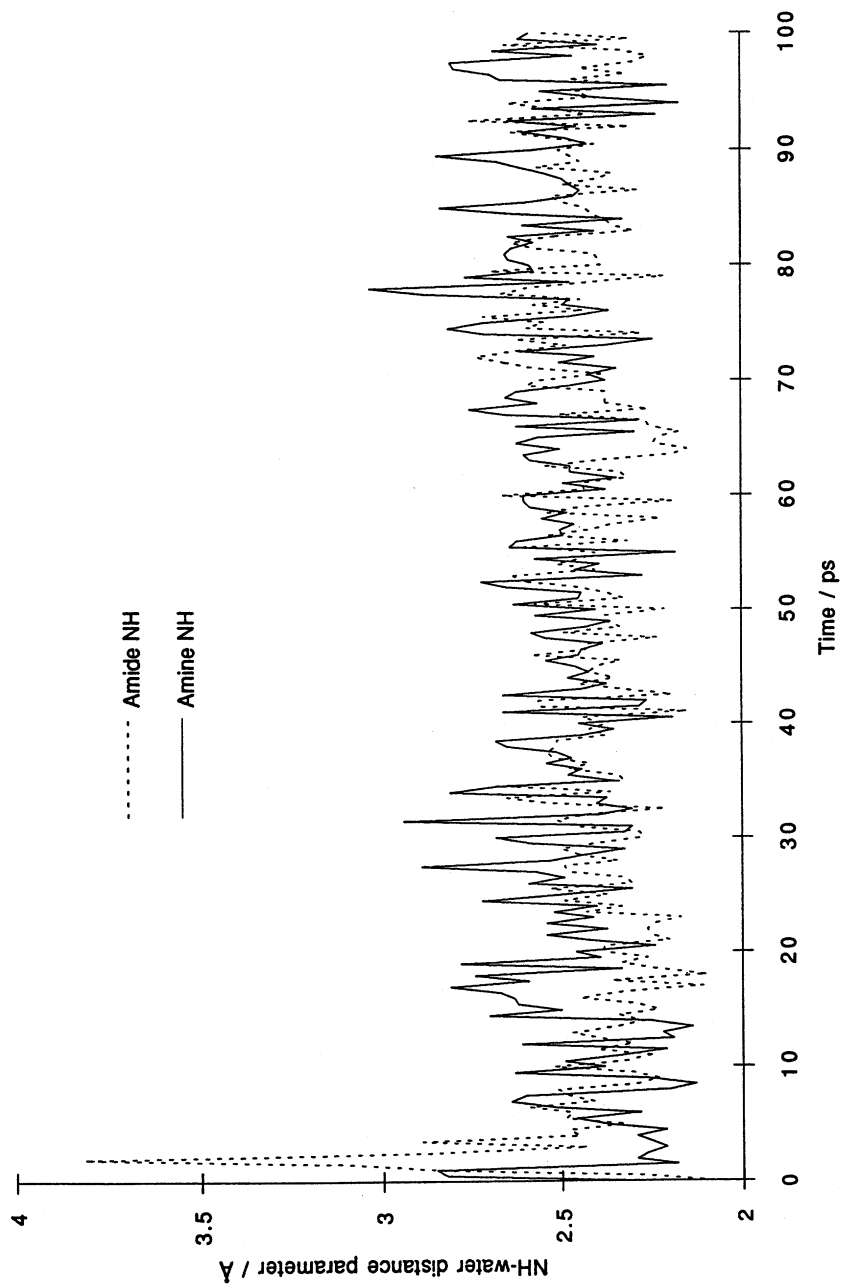


**Figure 11.** Variation of *N*-phenyl uronamide -NH $\leftrightarrow$ H<sub>2</sub>O distances as a function of simulated time in DMSO.

### Acknowledgements

Some of this research was funded by a grant from the U.S.-Israel Binational Agricultural Research and Development Fund (BARD).

---

Reference to a brand or firm name does not constitute endorsement by the U.S. Department of Agriculture over others of a similar nature not mentioned.

---

### Literature Cited

1. Laschi, F.; Pogliani, L. *Spectrosc. Lett.*, 1989, 22, 191.
2. Irwin, P.; Pfeffer, P.; Doner, L.; Lillie, T.; Frey, M. *J. Carbohydr. Chem.*, 1990, 9, 269.
3. Irwin, P.; Pfeffer, P.; Doner, L.; Ferretti, J. *J. Carbohydr. Chem.*, 1993, 12, 63.
4. DeTar, D.; Silverstein, R.; Rogers, F. *J. Am. Chem. Soc.*, 1966, 88, 1024.
5. Hoare, D.; Koshland, D. *J. Biol. Chem.*, 1967, 242, 2447.
6. R. L. Taylor and H. E. Conrad, *Biochem.*, 1972, 11, 1383.
7. Irwin, P.; Sevilla, M.; Osman, S. *Macromol.*, 1987, 20, 1222.
8. Haupt, E. *J. Magn. Resonance*, 1982, 49, 358.
9. Forsén, S.; Hoffman, R. *J. Chem. Phys.*, 1963, 39, 2892.
10. Shoubridge, A.; Briggs, R.; Radda, G. *FEBS Lett.*, 1982, 140, 288.
11. Balaban, R.; Kantor, H.; Ferretti, J. *J. Biol. Chem.*, 1983, 258, 12787.
12. King, G.; Warshel, A. *J. Chem. Phys.*, 1989, 91, 3647.
13. Clark, M.; Cramer, R.; van Opdenbosch, N. *J. Comput. Chem.*, 1989, 10, 982.
14. Gasteiger, J.; Marsili, M. *Tetrahedron*, 1980, 36, 3219.
15. Otting, G.; Wüthrich, K. *J. Am. Chem. Soc.*, 1989, 111, 1871.
16. Bothner-By, A.; Stephens, R.; Lee, J.; Warren, C.; Jeanloz, R. *J. Am. Chem. Soc.*, 1984, 106, 811.
17. Willem, R. *Prog. NMR Spectrosc.*, 1987, 20, 1.
18. van de Ven, F.; Janssen, H.; Gräslund, A.; Hilbers, C. *J. Magn. Resonance*, 1988, 79, 221.
19. Macura, S.; Ernst, R. *Mol. Phys.*, 1980, 41, 95.
20. Suter, D.; Ernst, R. *Phys. Rev. B*, 1985, 32, 5608.
21. Kumar, A.; Wagner, G.; Ernst, R.; Wüthrich, K. *J. Am. Chem. Soc.*, 1981, 103, 3654.
22. Kalk, A.; Berendsen, H. *J. Magn. Resonance*, 1976, 24, 343.
23. Hull, W.; Sykes, B. *J. Chem. Phys.*, 1975, 63, 867.
24. Bax, A.; Davis, D. *J. Magn. Resonance*, 1985, 63, 207.